HHS Public Access

Author manuscript

Cell. Author manuscript; available in PMC 2016 May 21.

Published in final edited form as:

Cell. 2015 May 21; 161(5): 999–1011. doi:10.1016/j.cell.2015.05.011.

Treatment of Obesity with Celastrol

Junli Liu[1,#], **Jaemin Lee**[1,#], **Mario Andres Salazar Hernandez**[1], **Ralph Mazitschek**[2,3], and **Umut Ozcan**[1,*]

[1]Division of Endocrinology, Boston Children's Hospital, Harvard Medical School, Boston, Massachusetts, 02130, USA

[2]Massachusetts General Hospital, Center for Systems Biology, Boston, MA 02114, USA

[3]The Broad Institute of Harvard and Massachusetts Institute of Technology, Cambridge, MA 02142, USA

SUMMARY

Despite all modern advances in medicine, an effective drug treatment of obesity has not been found yet. Discovery of leptin two decades ago created hopes for treatment of obesity. However, development of leptin resistance has been a big obstacle, mitigating a leptin-centric treatment of obesity. Here, by using *in silico* drug screening methods we discovered that Celastrol, a pentacyclic triterpene extracted from the roots of *Tripterygium Wilfordi* (Thunder of God Vine) plant, is a powerful anti-obesity agent. Celastrol suppresses food intake, blocks reduction of energy expenditure and leads up to 45% weight loss in hyperleptinemic diet-induced obese (DIO) mice by increasing leptin sensitivity, but is ineffective in leptin-deficient (*ob/ob*) or leptin receptor-deficient (*db/db)* mouse models. These results indicate that Celastrol is a leptin sensitizer and a promising agent for the pharmacological treatment of obesity.

INTRODUCTION

In 2008, the World Health Organization (WHO) estimated that 1.4 billion adults worldwide were overweight; of these, 200 million men and 300 million women were obese (Finucane et al., 2011). It is predicted that more than one billion people in the world will be obese by 2030 (Kelly et al., 2008). Obesity is a major cause for the development of debilitating conditions such as type 2 diabetes, cardiovascular disease, hypertension, and non-alcoholic steatohepatitis, all of which reduce life quality as well as life span (Olshansky et al., 2005).

*Correspondence: umut.ozcan@childrens.harvard.edu.
#These authors contributed equally to this work.

AUTHOR CONTRIBUTION

UO and RM came up with the idea to investigate compounds that have similar gene expression to 4-PBA by using CMAP. UO directed this and subsequent analyses and picked celastrol as a candidate for the treatment of diabetes and obesity. JL (Junli Liu), JL (Jaemin Lee) and MASH performed experiments under the direction of UO. Data were analyzed by UO, JL, and JL. The majority of the manuscript was written by UO with some help from JL and JL.

Nutritional and hormonal inputs from the periphery to the central nervous system (CNS) are interpreted by a complex neuronal circuitry, which maintains energy balance in the organism (Dietrich and Horvath, 2013; Myers et al., 2010). Leptin is an adipocyte-derived hormone, which is the main messenger that carries information about peripheral energy stores to the CNS (Dietrich and Horvath, 2013; Myers et al., 2010). The historic discovery of leptin by Friedman and co-workers two decades ago opened a new chapter with regard to the possibility of developing a treatment for obesity (Halaas et al., 1995; Zhang et al., 1994). However, initial hopes for leveraging leptin's anorectic effect for treating obesity quickly diminished, as it became clear that despite the presence of very high levels of circulating leptin in murine models of obesity and in obese humans, the hormone is ineffective in creating satiety and suppressing food intake (Considine et al., 1996; Frederich et al., 1995). Furthermore, while exogenously administered leptin does suppress food intake and reduce body weight in lean mice, it is ineffective in diet-induced obese (DIO) mice (Halaas et al., 1997). These findings led to the notion that obesity is a condition of leptin resistance, or leptin insensitivity (Considine et al., 1996; Frederich et al., 1995). Despite longstanding research efforts, drugs that can alleviate leptin resistance have not yet been found.

Perturbations of Endoplasmic reticulum (ER) homeostasis, predominantly triggered by the accumulation of unfolded proteins, lead to the development of a condition referred to as ER stress (Lee and Ozcan, 2014; Park and Ozcan, 2013; Ron and Walter, 2007), and activate a complex signaling cascade called the unfolded protein response (UPR) (Ron and Walter, 2007).

We have previously shown that ER stress is tightly linked to the pathophysiology of several metabolic diseases (Ozcan et al., 2004; Ozcan et al., 2006), including obesity (Ozcan et al., 2009; Ozcan et al., 2004). Previous observations documented that increased ER stress in the brain plays a central role in the development of leptin resistance, and consequently of obesity (Ozcan et al., 2009). Specifically, depletion of X-Box Binding Protein 1 (XBP1) from neurons leads to increased ER stress, severe hyperleptinemia, leptin resistance, and obesity (Ozcan et al., 2009). On the other hand, overexpression of spliced form of XBP1 (XBP1s) in *in vitro* and *in vivo* settings *increases* leptin sensitivity (Ozcan et al., 2009; Williams et al., 2014).

In parallel with these findings, chemical chaperones such as 4-phenyl butyrate (4-PBA) and Tauroursodeoxycholic acid (TUDCA), which are agents that improve ER function and decrease ER stress, increase leptin sensitivity, although rather weakly (Ozcan et al., 2009; Ozcan et al., 2006).

Experimental findings indicate that the use of different manipulations that interfere with the ER system with the goal of reducing ER stress could have distinct outcomes. For example, transcription factors such as XBP1s or activating transcription factor-6 (ATF6) increase the expression of chaperones and reduce ER stress (Ron and Walter, 2007), while expression of sarco(endo)plasmic reticulum Ca^{2+} ATPase 2b (SERCA2b) in the liver reduces ER stress (Park et al., 2010), but without altering the expression of chaperones. In both situations, ER stress is reduced, but in one case it is accompanied by upregulation of chaperone expression, and in the other it is not. Furthermore, chemical chaperones can also decrease ER stress,

however this reduction may be accompanied by a decreased chaperone expression (de Almeida et al., 2007). Thus, depending on the specific manipulation, the shift from a stressed to a non-stressed ER could have different homeostatic outcomes, including increased, unaltered or decreased expression of ER stress-related genes. This means that homeostatic ER conditions can manifest along with the up or down regulation of the same set of genes.

In our current work, we used an alternative approach to identify small molecules that could increase leptin sensitivity and treat obesity. We reasoned that rather than targeting a single molecule in the UPR signaling pathway, we should utilize the outcome of a variety of interventions that reduce ER stress; and that we should use these outcomes of homeostatic ER conditions to search for small molecules that can create the same outcomes.

Connectivity Map (CMAP) comprises a database and associated software that is produced by the Broad Institute, and is composed of whole genome gene expression profiles derived from human cell lines that were treated with more than a thousand small molecules (Lamb et al., 2006). The software can compare two sets of genes, which are desired by user to be up-regulated and down regulated (up-list and down-list, respectively), with the whole CMAP database. CMAP can thus be utilized to identify small molecules that create gene expression patterns similar to the ones being searched for.

In our current work, we have created gene expression signatures by utilizing the microarray data obtained following various interventions to relieve ER stress in a number of tissues; we then used these signatures to identify small molecules that can increase leptin sensitivity and thereby offer a treatment for obesity.

RESULTS

Use of Transcriptional Profiling to Identify Small Molecule Leptin Sensitizers

4-PBA reduces ER stress, even in the absence of XBP1 (Ozcan et al., 2006), suggesting that each manipulation establishes ER homeostasis via independent pathways. Based on this, we first sought to determine the whole genome gene expression profile of livers that were obtained either from 4-PBA-treated mice, or from obese mice with liver-specific overexpression of XBP1s. These expression profiles from liver were selected for two reasons: i) Both of these conditions were representation of a homeostatic ER state that had been established on a previously stressed condition through different mechanisms, and ii) CMAP is based on data obtained from cell lines, which led us to reason that inclusion of liver microarrays would increase our chances of identifying small molecules, because hypothalamus is a highly specialized tissue.

To determine the 4-PBA-regulated transcriptome, we treated *ob/ob* mice and their lean controls either with vehicle or 4-PBA, then dissected out the livers from both groups and extracted RNA for microarray analysis. In parallel, to identify the XBP1s-regulated expression liver profile in obese mice, XBP1s-expressing adenovirus (Ad-XBP1s) or a control LacZ-expressing adenovirus (Ad-LacZ) was injected into the tail vein of *ob/ob* mice, and subsequently the liver RNA was isolated and prepared for microarray analysis.

We first determined the fold changes in levels of gene expression in livers from 4-PBA- vs. vehicle-treated lean or o*b/ob* mice, following which the same analysis was done in XBP1s- vs. LacZ-expressing *ob/ob* mice. From each of the above three experimental groups, we selected 50 up-regulated and 50 down-regulated genes (Figure 1A and 1B) and converted the mouse gene identifiers for our probe annotations to human gene identifiers. The final lists of genes that were analyzed as gene signatures in CMAP were of varying lengths due to this conversion (Figure S1).

We first obtained individual enrichment scores for the three gene signatures (fold-changes created by XBP1s overexpression in the liver of obese mice, following 4-PBA treatment in the liver of lean or obese mice). However, as discussed above, relieved ER stress can manifest as increased or decreased expression of related genes - in other words, each distinct condition of relieved ER stress may be positively or negatively correlated to levels of gene expression, which would correspond to positive or negative enrichment scores, respectively. Therefore we calculated the absolute values of enrichment scores, and used the *absolute enrichment score* in our analysis.

At the outset, we first analyzed the absolute enrichment score of CMAP results that were obtained by using the gene array of lean mice, treated with 4-PBA. The results from this analysis led to identification of Celastrol as the most promising candidate, which initiated the research on Celastrol (Figure 1C). Subsequently, after obtaining the distribution of the absolute enrichment scores for all small molecules in CMAP for the three gene signatures (Figure 1C), we also used a new method to rank the small molecules with a single dimensional metric, which is calculated from the three absolute enrichment scores (Figure 1D); this metric was defined as the *absolute product score*, and it represents the value of the highest score from the combination of the three enrichment scores. This algorithm also yielded Celastrol as the top ranking small molecule and proved the initial observations (Figure 1E).

We subsequently also used expression profiles from the hypothalamus, a tissue that is vital for leptin action and is the major site for leptin resistance. We first compared the negative or positive alterations in the gene expression profile of the hypothalamus of DIO mice to those of lean controls. The 50 most up- and down-regulated genes in the hypothalami of DIO versus lean mice were used to generate an obesity-related hypothalamic gene expression signature, referred to here as the *hypothalamic obesity signature* (Figure 1F and 1G).

Next, to determine chemical chaperone-induced changes in the pattern of gene expression in the hypothalamus, DIO mice were divided into three subgroups, and treated with saline, 4-PBA or TUDCA for seven days. Fold changes (relative to control) in the levels of gene expression in the hypothalami of 4-PBA- or TUDCA-treated mice were calculated. To generate one signature related to chemical chaperones, we took the geometric mean of fold changes for each gene in the 4-PBA- and TUDCA-treated groups (Figure 1F and 1G); we defined these as the *hypothalamic chaperone signatures* (Figure 1G). The absolute value of the enrichment scores for each of the two signatures was calculated by CMAP (Figure 1H). The absolute product score again ranked Celastrol as one of the top compounds in the database (Figure 1I). As seen from the combined distribution of the absolute product scores

for the liver and hypothalamus shown in Figure 1J, Celastrol was the highest scoring small molecule (once the absolute product scores of liver and hypothalamus experiments had been further analyzed by multiplication of these two scores) (Figure 1K).

Celastrol is a pentacyclic triterpene extracted from the *Tripterygium Wilfordi* (Thunder of God Vine) plant (Corson and Crews, 2007). The plant itself has a long history of human use in traditional Chinese medicine, typically for rheumatoid arthritis, but we have found no reports of Celastrol by itself having been administered to humans. Celastrol reportedly has anti-cancer effects both *in vitro* and *in vivo* (Corson and Crews, 2007)

Celastrol Ameliorates Obesity in HFD-Fed Obese Mice

DIO mice were either treated with vehicle or Celastrol intraperitoneally. Administration of Celastrol significantly reduced the body weight of DIO mice, from 47.53±1.0 g to 35.43±0.97 g (on day 1 vs. day 15 of treatment, $p<0.001$), after which the body weights were stabilized. At the end of the third week, body weight of Celastrol-receiving DIO mice reached 34.38±1.06 g (Figure 2A), corresponding to a 27.67±1.48% weight loss relative to their initial weights (Figure 2B). The body weight of vehicle-treated control mice showed no alterations. During the first week of trial, the daily food intake for the control group was 2.06±0.11 g, and was reduced to 0.43±0.12 g in the Celastrol-treated group, corresponding to a 79% reduction (Figure 2C and S2A). Reduction in food intake seen during the first week gradually disappeared and was normalized to control levels by the end of the three-week period (data not shown). This increase in the food intake during the last week was inversely correlated to the levels of circulating leptin, which steadily decreased and reached close-to-lean levels by the end of the three-week treatment period (Figure 2D). Celastrol treatment did not alter the lean mass of DIO mice relative to the vehicle-treated control group (Figure 2E). However, the fat percentage of Celastrol-treated mice was significantly (41.5%) lower than that of vehicle-treated group (Figure 2F).

As opposed to DIO mice, lean mice have very low levels of circulating leptin levels. Based on the fact that Celastrol-induced weight loss is much more potent at the beginning of the treatment period, when the DIO mice are hyperleptinemic, and that the response of the mice to Celastrol ceases as plasma leptin levels drop, we reasoned that Celastrol would have minimal effects in lean mice. Consistent with our expectations, Celastrol administration did not significantly reduce the body weight of lean mice at the doses that it was effective in DIO mice (Figure 2G and 2H). On the contrary, Celastrol-treated lean mice continued to gain weight as the control group (Figure 2G and 2H). Furthermore, the food intake of vehicle- or Celastrol-treated lean mice was the same (Figure 2I and S2B), and plasma leptin levels of lean mice were not altered during the treatment period (Figure 2J). We also did not detect any changes in the lean mass (Figure 2K) or fat percentage (Figure 2L) of lean mice treated with Celastrol. These findings further supported the possibility that Celastrol is a leptin sensitizer. Furthermore, we have also administered vehicle or Celastrol to wt mice that were kept on chow or HFD in two different cohorts for 195 and 216 days (Figure S2I and S2J). This long-term chronic administration has shown that first, Celastrol does not create toxic effect in mice and secondly it also suppresses development of obesity.

Celastrol Is a Leptin Sensitizer

If Celastrol is, indeed, a true leptin sensitizer, it should either have no effect, or a minimal effect, in *ob/ob* or *db/db* mice, both of which lack leptin action. We therefore tested the effect of Celastrol on *ob/ob* and *db/db* mice. Vehicle-treated *db/db* mice gained weight during the course of the experiment (Figure 3A and 3B). Importantly, treatment of *db/db* mice with Celastrol did not induce any weight loss, and the mice gained similar amounts of weight as did the vehicle-treated mice (Figure 3A); in fact, at the end of the treatment period, the body weight of *db/db* mice receiving Celastrol treatment was 14.01±0.68% heavier than their initial bodyweight (Figure 3B). The food intake (Figure 3C and S2C), lean mass (Figure 3D), fat percentage (Figure 3E) and the leptin levels (Figure 3F) of the vehicle- vs. Celastrol-treated *db/db* mice were unchanged between the two groups.

We next investigated the effect of Celastrol on *ob/ob* mice. Vehicle-treated *ob/ob* mice continued to gain weight (Figure 3G and H). Administration of Celastrol to *ob/ob* mice led to a slight decrease in the body weight during the first week of treatment, but this decrease was rapidly compensated, and no significant difference in the body weights of animals in the two groups was detected after the trial (Figure 3G). In fact, there was a slight *increase* in their body weight at the end of the trial (Figure 3H). Food intake of the *ob/ob* mice showed a slight but significant decrease during the first week in the majority of the independent experimental cohorts (data not shown), but this reduction, despite continuing presence of obesity of *ob/ob* mice, was rapidly normalized in the second week of treatment and thereafter (Figure 3I and S2D). Furthermore, lean mass (Figure 3J), and the fat percentage (Figure 3K) of *ob/ob* mice were also not affected by Celastrol treatment.

Oral Administration of Celastrol Also Has a Strong Anti-Obesity Effect in DIO Mice

To investigate whether Celastrol also exerts its anti-obesity effect when it is administered orally, we also administered Celastrol by oral gavage. Figures 4A and 4B show that oral administration of vehicle for three weeks did not alter the body weights of DIO mice. However, oral administration of Celastrol had a robust effect on body weight, reducing it from 49.85±0.97 g on day 1 to 27.15±1.37 g on day 22 ($p<0.001$), corresponding to a 45.4±3.46% decrease relative to their initial bodyweights (Figure 4B). The food intake of DIO mice was also significantly reduced when compared to the vehicle-treated group (Figure 4C and S2E). Oral administration of Celastrol to lean (Figure 4D–F and S2F), *db/db* (Figure 4G–I and S2G) and *ob/ob* (Figure 4J–L and S2H) mice did not induce a significant change in body weight or food intake compared to their respective control groups.

Celastrol Potentiates Leptin's Effect

We reasoned that administration of exogenous leptin to lean mice that were pre-treated with Celastrol should create a stronger outcome compared to administration of leptin to a vehicle-pretreated control, if the absence of effect of Celastrol in lean mice were due to low levels of circulating leptin. We thus administered lean mice either vehicle, or Celastrol, and subsequently, injected saline or a bolus dose of leptin to each group. Figure 5A shows that leptin administration to lean mice (Vehicle+Leptin) led to a significant decrease in food intake (corresponding to a 41% decrease in Vehicle+Leptin over the Vehicle+Saline group). Lean mice that received Celastrol plus leptin, consumed less food than any of the other

groups – this leptin-induced suppression of food intake in the presence of Celastrol corresponded to a 62% decrease, when compared to the food intake of the Celastrol+Saline group (Figure 5A).

Leptin administration to lean mice (Vehicle+Leptin) resulted in a significant decrease in the body weight (Vehicle+Saline vs. Vehicle+Leptin, $p<0.01$), but Celastrol alone (Celastrol +Saline) did not cause a significant change in the body weight of lean mice (Vehicle+Saline vs. Celastrol+Saline, $p=0.10$). Leptin administration to lean mice that were pre-treated with Celastrol led to a 1.87±0.32 g loss in bodyweight. These results show that the average leptin-induced reduction in body weight for Celastrol-pre-treated mice was 1.63 g, in contrast to the 0.63 g decrease in mice that were pre-treated with vehicle, suggesting that Celastrol potentiates the effect of leptin in reducing weight in lean mice (Figure 5B).

To investigate whether Celastrol also acutely potentiates the anorectic and weight-reducing effects of *exogenous* leptin in DIO mice, we tested the response of these animals to leptin in the presence and absence of Celastrol. Administration of leptin to DIO mice did not significantly alter their food intake, compared to the control group. Celastrol treatment alone decreased the food intake of DIO mice (Vehicle+Saline vs. Celastrol+Saline, $p<0.001$). And administration of leptin to DIO mice that were pre-treated with Celastrol (Celastrol+Leptin), led to a further reduction in food intake relative to the Celastrol+Saline group ($p<0.01$) (Figure 5C). Furthermore, treatment with leptin alone did not significantly change the body weights of DIO mice (Figure 5D), while Celastrol treatment led to a 0.86±0.15 g decrease in body weight of DIO mice ($p<0.001$) (Figure 5D). Administration of leptin in the presence of Celastrol (Celastrol+Leptin group) documented that Celastrol further augmented the negative effect of leptin on body weight; DIO mice in the Celastrol+Leptin group lost 1.42±0.19 g of body weight, which was significantly lower than all of the other groups (Figure 5D).

To provide additional physiological proof that Celastrol acts as a leptin sensitizer, we tested whether additional Celastrol treatment further upregulates leptin action in *ob/ob* mice. As shown in Figure 5E, low dose of leptin by itself created no significant differences in the body weight gain of the *ob/ob* mice. However, administering the same dose of leptin in the presence of Celastrol led to a pronounced weight loss during the course of the treatment, with *ob/ob* mice losing 15.36±2.61% of their initial body weight ($p<0.001$ vs. all other groups) (Figure 5E). Co-administration of leptin and Celastrol led to a two-fold greater suppression of food intake (leptin-induced % suppression of food intake in vehicle vs. Celastrol groups, $p<0.001$), suggesting that Celastrol potentiates the anorectic effect of leptin even in *ob/ob* mice (Figure 5F).

Celastrol Activates the Hypothalamic Leptin Receptor-Stat3 Pathway in DIO Mice

We next investigated the Leptin receptor signaling network after Celastrol treatment. To address whether Celastrol increases hypothalamic leptin sensitivity, we analyzed how acute Celastrol administration influences leptin-stimulated $STAT3^{Tyr705}$ phosphorylation in DIO mice at a time when the mice are still obese and hyperleptinemic.

Injection of this hormone in vehicle-treated DIO mice did not lead to a significant increase in Stat3^{Tyr705} phosphorylation (Figure 6A and 6B), but Celastrol treatment alone did lead to a significant increase in basal levels of Stat3^{Tyr705} phosphorylation in the hypothalamus (Figure 6A and 6B). However, when leptin was administered to DIO mice that were pre-treated with Celastrol, the levels of p-STAT3^{Tyr705} in the hypothalamus increased even further (Figure 6A and 6B), indicating that treatment of DIO mice, with even a single dose of Celastrol, was sufficient to increase leptin sensitivity.

We next investigated the hypothalamic mRNA levels of pro-opiomelanocortin (*Pomc*), Agouti-related peptide (*Agrp*), and Neuropeptide Y (*Npy*). Surprisingly, we did not find any difference in the mRNA levels of *Pomc* between vehicle and Celastrol-treated mice (Figure 6C). Furthermore, we have found that *Agrp* expression levels, completely contrary to general expectations, were significantly increased (Figure 6D). However, *Npy* mRNA levels were not altered (Figure 6E). In addition, suppressor of cytokine signaling 3 (*Socs3*) expression level was significantly increased in the Celastrol-treated DIO mice when compared with the control group (Figure 6F).

Celastrol Reduces ER Stress in the Hypothalamus

We next investigated the effect of Celastrol on the status of ER stress in the hypothalamus of DIO mice. Treatment of mice with Celastrol led to a significant decrease in PERK phosphorylation, indicating that Celastrol reduces ER stress (Figure 6G and S3A–H). Moreover, we also treated Tuberous Sclerosis Complex-2 (TSC2) knock out (TSC2$^{-/-}$) mouse embryo fibroblasts (MEF) with Celastrol. TSC2$^{-/-}$ cells were previously shown to have intrinsic ER stress (Ozcan et al., 2008). Treatment of TSC2$^{-/-}$ cells with Celastrol has shown that Celastrol also reduces PERK phosphorylation and consequently ER stress in this *in vitro* system (Figure S3I). Furthermore, analysis of SERCA2b levels also showed a significant reduction in the hypothalamus of Celastrol-treated mice (Figure 6H and 6I).

We next investigated the mRNA levels of XBP1s, various ER chaperones and mitofusins (*Mfn1* and *Mfn2*). However, we did not see any alterations in the mRNA levels of these genes (Figure S3J and S3K).

Celastrol has been also suggested to inhibit NF-κB signaling pathway (Lee et al., 2006). Determining the mRNA levels of various target genes of NF-κB pathways, showed no difference in the hypothalamus of vehicle- or Celastrol-treated mice (Figure S4A). Celastrol also has been proposed as a heat shock protein 90kDa (HSP90) inhibitor (Hieronymus et al., 2006). HSP70 protein levels is an indicator of HSP90 activity and inhibition of HSP90 leads to increase in HSP70 protein levels (Neckers, 2007). However, we did not find any increase in HSP70 protein levels, on the contrary there was a slight decrease. (Figure S4B and S4C).

Energy Homeostasis in Mice Treated with Celastrol

Leptin is reported to maintain high-energy expenditure, even though it reduces food intake (Halaas et al., 1995). Based on the above data, we reasoned that Celastrol, despite its robust effects on food intake and bodyweight, would enhance energy expenditure and lead to the utilization of fat as the main energy source. We thus measured metabolic parameters (energy

expenditure (EE) and respiratory exchange ratio (RER), and levels of physical activity) in vehicle- and Celastrol-treated mice. No differences were seen in EE between vehicle- and Celastrol-treated groups in the dark cycle (Figure 7A). However, EE of the Celastrol-treated mice was higher in the light cycle (Figure 7A). Also, RER values were significantly decreased in Celastrol-treated DIO mice both in the dark and light cycles (Figure 7B). Levels of physical activity during the dark phase in DIO mice were significantly reduced as a result of Celastrol administration, but no differences were observed in the light phase (Figure 7C). It is possible that the reduced physical activity in the Celastrol-treated group during the dark cycle, is due to decreased food-searching behavior.

Metabolic parameters were also measured in lean mice. EE in the dark cycle was slightly but significantly reduced in Celastrol-treated lean mice (Figure 7D). Relative to vehicle-treatment, Celastrol administration did reduce the RER values during the dark phase (Figure 7E). Furthermore, Celastrol led to a significant reduction in their physical activity in the dark cycle compared to the control group (Figure 7F). We also analyzed how Celastrol treatment affected the *ob/ob* and *db/db* mouse models. Surprisingly, acute administration of Celastrol to *ob/ob* mice led to a slight but significant reduction in EE in both cycles (Figure 7G). RER values were also significantly reduced in the dark phase (Figure 7H), which were accompanied with a reduction of physical activity in the dark phase (Figure 7I). EE was also significantly reduced in Celastrol-treated *db/db* mice (Figure 7J). However, RER values and physical activity were not altered in the *db/db* mice (Figure 7K and 7L). The above metabolic chamber measurements were obtained following 12–60 hours of Celastrol-treatment. Because plasma leptin levels in DIO mice return to almost normal levels following chronic Celastrol treatment, we made additional metabolic chamber measurements after chronic (3 weeks) vehicle or Celastrol administration. Analysis of EE, RER, and physical activity in DIO mice showed no differences during the third week of treatment (Figure S5A–C). In addition, such chronic treatment also yielded no differences in EE, RER, or the physical activity of lean, *ob/ob* or *db/db* (Figure S5D–L) mice.

We next compared the metabolic profiles of Celastrol-treated DIO mice and their pair-fed, vehicle-treated controls. Vehicle-treated DIO mice were subdivided into two groups; the first was allowed to eat *ad libitum* (vehicle group), while the other was pair-fed with the Celastrol group (pair-fed group). Figure S6A shows that during the three-day period when pair-feeding experiments were performed, the average daily food intake of the Celastrol mice was the same as for the pair-fed groups. Treatment of DIO mice with Celastrol did not alter the EE in the dark cycle and there were no difference among the three groups in the dark cycle (Figure S6B). In the light cycle, EE of Celastrol-treated mice showed slight but not a significant increase when compared with the vehicle-treated group. However, Celastrol-treated group had significantly higher EE than the pair-fed group in the light cycle (Figure S6B). RER values were significantly decreased in the Celastrol-treated group compared to both vehicle and pair-fed groups in both dark and light cycles. However, the pair-fed groups' RER, when compared to the vehicle-treated control group, did not show any alterations (Figure S6C). The physical activity of the Celastrol-treated mice was again significantly lower than the vehicle-treated group (Figure S6D), but no reduction in physical activity was seen for the pair-fed group (Figure S6D). Importantly, the Celastrol-treated

group underwent significantly greater weight loss than did the vehicle-treated and pair-fed groups (Figure S6E).

We next analyzed the liver from the mice that were treated with either vehicle or Celastrol for three weeks and documented that livers of DIO mice treated with Celastrol were virtually non-differentiable from sections taken from the lean mice (Figure S6F), which indicates that Celastrol treatment in DIO mice also leads to elimination of hepatic steatosis.

Plasma levels of alanine transaminase (ALT) and aspartate aminotransferase (AST) (Figure S6H and S6I) showed significant reductions in both groups, pointing to improved liver function. Furthermore, total plasma cholesterol level was significantly decreased in Celastrol-treated DIO mice (Figure S6J). Plasma levels of triiodothyronine (T3) in vehicle- and Celastrol-treated DIO mice and documented that T3 levels were decreased, indicating that Celastrol does not induce hyperthyroidism (Figure S6K).

Celastrol Enhances Glucose Homeostasis in DIO Mice

We next investigated whether Celastrol can also improve glucose homeostasis in DIO mice. Following treatment of DIO mice with vehicle or Celastrol for one week, we performed a glucose tolerance test (GTT). Clearance of glucose from the circulation during GTT was significantly faster in Celastrol-treated mice than in the vehicle-treated mice (Figure S7A and S7B). Two weeks of Celastrol treatment also improved insulin sensitivity in DIO mice, which were analyzed by an insulin tolerance test (ITT) (Figure S7C and S7D). The blood glucose level at six-hour fasting was also significantly lower in the Celastrol-treated mice compared to the vehicle-treated group (Figure S7E). And when blood glucose levels of Celastrol-treated DIO mice were compared to those in the pair-fed group, the Celastrol-treated mice had significantly lower levels (Figure S6G). In addition, plasma insulin levels were significantly decreased in Celastrol-treated DIO mice relative to the control group (Figure S7F).

Analysis of glucose tolerance in lean mice showed a significant improvement following one week of Celastrol treatment (Figure S7G and S7H). But we did not detect any differences in ITT (Figure S7I and S7J), six-hour fasting blood glucose levels (Figure S7K), or plasma insulin levels (Figure S7L) in vehicle- vs. Celastrol-treated lean mice. Celastrol treatment at this dose (100 μg/kg) in *db/db* or *ob/ob* mice did not lead to improvement in any of the parameters (Figure S7M–X).

DISCUSSION

Organisms that have developed powerful mechanisms to store energy and use it efficiently have likely passed through a stringent natural selection process during evolution (Dietrich and Horvath, 2013; Friedman, 2009; Myers et al., 2010). And correspondingly, systems that have evolved to communicate the amount of energy stored in the body to the brain are among the most critical for surviving in nature. Leptin was the first and most powerful hormone identified in relation to the control of energy metabolism and to communicating information about peripheral energy sufficiency to the brain. Reduction in the physiological concentrations of circulating leptin in a starvation state creates a very powerful stimulus for

food consumption, and signals a need for the body to increase its energy stores, and at the same time to reduce energy expenditure for multiple physiological functions. Indeed, the *ob/ob* and *db/db* mouse models, all of which lack leptin action, develop morbid obesity due to severely increased food intake and reduced energy expenditure (Coleman, 1978).

Despite very high concentrations of leptin in the circulation in obesity, the hormone can neither suppress food intake nor increase energy expenditure. Instead, obesity is characterized by hyperphagia and reduced energy expenditure, reminiscent of a leptin-deficient condition (Friedman, 2004). These observations led to the notion that obesity is a leptin-resistant condition. But the absence of definitive evidence on the effectiveness of using high levels of circulating leptin to treat obesity has created a long standing-debate about whether or not the condition of leptin resistance actually exists.

Here we have used an unconditional *in silico* screening approach to look for small molecules that increase leptin sensitivity. We developed this strategy primarily based on our previous observations that increased hypothalamic ER stress is a major causative factor in the development of leptin resistance and obesity. ER stress signaling is a highly complex and one of the most central signaling pathways in the cell. Considering that the targeting of single molecules for treatment of obesity has failed to lead to the discovery of effective obesity drugs, we did not try to target the "*usual suspects*" (such as JNK, ATF4 or others) in the ER stress pathway. Instead we focused primarily on homeostatic ER conditions, which were specifically established on a previous condition that was characterized with ER stress. As such, we used a variety of tissues and a number of different manipulations to reduce ER stress, and determined the outcome of these manipulations in terms of gene expression profiling. We then used these expression profiles to search for small molecules, which have ability to create the same expression profiles. However, considering the different possibilities in gene expression profiles of reduced ER stress conditions, we did not use the basic enrichment scores provided by CMAP but added another component to the analysis by converting these enrichments scores to *absolute* enrichment scores for the analysis. Furthermore, subsequently, yet another layer was added to this initial analysis: we used all the absolute enrichment scores to determine the small molecule which had the highest score in terms of its similarity to all six expression profiles that were used in the screening. Celastrol again had the highest score, with a high distance to all other molecules in the CMAP database.

A true leptin sensitizer should, above all, be effective in hyperleptinemic and leptin-resistant DIO mice, and should have minimal or no effects in lean, *ob/ob* or *db/db* mice. Furthermore, a putative leptin sensitizer should reduce food intake, should not lead to a reduction in energy expenditure as seen in starvation conditions, and its effect should gradually diminish as the obese mice lose weight and leptin levels return to normal. Celastrol meets all of these specifications. While administration of Celastrol to hyperleptinemic and leptin-resistant DIO mice was effective in decreasing food consumption, and in reducing body weight by up to 45%, minimal effects were noted in the food intake and body weight of lean mice, or of *ob/ob* and *db/db* mice. And despite the major reductions in food intake and consequently in the bodyweight of Celastrol-treated DIO mice, lean mass in these animals was not altered, consistent with the notion that leptin-induced anorexia does not cause a reduction in lean

mass (as opposed to starvation-caused weight loss) (Halaas et al., 1995). More interestingly, Celastrol treatment in obese mice significantly decreased RER values relative to vehicle-treated obese controls or the pair-fed group, further indicating the increase in leptin sensitivity. All of these results provide evidence in support of a role for Celastrol in reducing obesity by increasing leptin sensitivity.

Additional evidence that Celastrol is a leptin sensitizer comes from experiments in which we analyzed the physiological and biochemical responses to exogenous leptin administration. Our hypothesis for the ineffectiveness of Celastrol in lean mice was the low levels of circulating leptin in this model. If this hypothesis is correct, increasing the circulating levels of leptin acutely in Celastrol-pretreated lean mice should have a greater effect than in a control group. Indeed, this was the case: we found that when Celastrol-pretreated lean mice were injected with leptin, food consumption and body weight were both significantly reduced relative to the vehicle-pretreated mice. Furthermore, despite the fact that Celastrol already utilizes the high levels of endogenous leptin, administration of a bolus dose of leptin also leads to a greater reduction in bodyweight of leptin-resistant DIO mice. And finally, in addition to these direct physiological responses, Celastrol also augmented the phosphorylation of $STAT3^{Tyr705}$ in the hypothalamus, an effect that was further enhanced by leptin injection.

Taken together, these observations document that Celastrol is a leptin sensitizer and clearly point to the existence of leptin resistance in obesity. The findings also make a strong case for the therapeutic potential of increasing the sensitivity of obese states to leptin.

How does Celastrol create the leptin sensitizing effect? We do not have a single molecule-based mechanistic explanation at the moment. Celastrol can be discovered by analyzing the effects of XBP1s and of the chemical chaperones (4-PBA and TUDCA); the findings were further enriched with the differential gene expression profile of the hypothalamus in DIO mice. Indeed, Celastrol significantly reduces PERK phosphorylation and SERCA2b protein levels, which all strongly indicates that ER stress is reduced and provide a direct mechanistic link between Celastrol, ER stress and leptin sensitization.

In addition, Celastrol has been shown to inhibit HSP90. HSP90 is one of the most abundant proteins in the cell and high levels of Celastrol were previously shown to inhibit HSP90. However, the doses that we used in mice do not inhibit HSP90, and HSP90 inhibition in our experimental setting is irrelevant for a mechanistic explanation for Celastrol action. Also, it has been suggested that high doses of Celastrol block NF-κB activity (Lee et al., 2006); however, analysis of the NF-κB target genes either did not show any alterations or we observed treatment-related *increases* in the levels of several genes that are also the target NF-κB (data not shown). While further studies are needed to unravel the exact mechanism of action(s) of Celastrol in increasing leptin sensitivity, the results that we obtained thus far clearly indicate that Celastrol's anti-obesity action cannot be attributed to either HSP90 or NF-κB inhibition.

Our approach in this study did not involve drug screening based on the targeting of single molecules. Rather, our experimental strategy was motivated by the long years of failure in

finding a treatment for obesity by a single target-based screenings. Our use of an unconditional alternative approach has uncovered a very potent anti-obesity molecule. The effect of Celastrol is more potent than reported for bariatric surgery in mice, with which weight loss is around 35–40% (Liou et al., 2013; Mokadem et al., 2014; Ryan et al., 2014). Obesity affects more people worldwide than any other debilitating disease. If Celastrol works in humans the way it does in mouse models, the outcome could be an effective therapeutic approach for treatment of obesity.

EXPERIMENTAL PROCEDURES

Whole genome gene expression studies

For liver whole genome gene expression study, ten-week-old lean male and ten-week-old *ob/ob* male mice orally received either saline (n=3 for each group) or 4-PBA (n=3 for each group; 1 g/kg, twice a day in 0.5 g/kg for ten days). After ten-day treatment, the liver was extracted and flash frozen in liquid nitrogen. Another group of ten-week-old *ob/ob* male mice were injected with 1×10^8 pfu (per g body weight) of adenoviruses that express β-galactosidase (Ad-LacZ) or mouse XBP1s (Ad-XBP1s) via the tail vein (n=3 for each group). One week after injection, all mice were fasted for six hours and the liver was extracted and stored in −80°C until further processing.

For hypothalamus whole genome gene expression study, hypothalami of DIO mice fed with HFD for 20 weeks and age-matched lean mice fed with chow diet for 20 weeks were collected and stored in −80°C for later processing (n=4 for each group). In another experiments, DIO mice fed with HFD for 16 weeks were administered with either saline, 4-PBA (1 g/kg/day) or TUDCA (150 mg/kg/day) for seven days and their hypothalami were collected, flash frozen in liquid nitrogen and stored in −80°C before processing.

RNAs from the liver of mice that were treated with vehicle or 4-PBA were analyzed on Illumina MouseRef-8 Expression BeadChips. RNA samples from the liver of mice that were injected with Ad-LacZ or Ad-XBP1s were analyzed on Affymetrix GeneChip Mouse Genome 430 2.0 Array. RNA samples from the hypothalamus of lean and DIO mice were analyzed on Affymetrix Mouse Gene 1.0 ST Array.

The microarray data obtained from experiments described above were used as queries for Connectivity Map (CMAP) after conversion into human homologues and detailed processes are described in the Extended Experimental Procedures.

Metabolic chamber measurements

Metabolic parameters of all mouse models (lean, DIO, *ob/ob* and *db/db*) were determined by using Columbus Instruments Comprehensive Lab Animal Monitoring System (CLAMS). Further experimental details can be found in the Extended Experimental Procedures and raw data for energy expenditure (EE), respiratory exchange ratio (RER), and ambulatory activity (X-Amb) can be found in supplemental data files S2 and S3.

Supplementary Material

Refer to Web version on PubMed Central for supplementary material.

Acknowledgments

We greatly appreciate the time of Morris F. White and Joseph A. Majzoub for critical reading of our manuscript and for their contributions and suggestions. We thank to Serkan Cabi, Isin Cakir and Safak Mert for their experimental contributions to this work. This work was mainly supported by the funds provided to UO from Department of Medicine, Boston Children's Hospital and also by grant R01DK098496 provided to U.O. by the National Institutes of Health, American Diabetes Association Career Development grant #7-09-CD-10 and support from Fidelity Biosciences Research Initiative.

References

Coleman DL. Obese and diabetes: two mutant genes causing diabetes-obesity syndromes in mice. Diabetologia. 1978; 14:141–148. [PubMed: 350680]

Considine RV, Sinha MK, Heiman ML, Kriauciunas A, Stephens TW, Nyce MR, Ohannesian JP, Marco CC, McKee LJ, Bauer TL, et al. Serum immunoreactive-leptin concentrations in normal-weight and obese humans. The New England journal of medicine. 1996; 334:292–295. [PubMed: 8532024]

Corson TW, Crews CM. Molecular understanding and modern application of traditional medicines: triumphs and trials. Cell. 2007; 130:769–774. [PubMed: 17803898]

de Almeida SF, Picarote G, Fleming JV, Carmo-Fonseca M, Azevedo JE, de Sousa M. Chemical chaperones reduce endoplasmic reticulum stress and prevent mutant HFE aggregate formation. The Journal of biological chemistry. 2007; 282:27905–27912. [PubMed: 17626021]

Dietrich MO, Horvath TL. Hypothalamic control of energy balance: insights into the role of synaptic plasticity. Trends in neurosciences. 2013; 36:65–73. [PubMed: 23318157]

Finucane MM, Stevens GA, Cowan MJ, Danaei G, Lin JK, Paciorek CJ, Singh GM, Gutierrez HR, Lu Y, Bahalim AN, et al. National, regional, and global trends in body-mass index since 1980: systematic analysis of health examination surveys and epidemiological studies with 960 country-years and 9.1 million participants. Lancet. 2011; 377:557–567. [PubMed: 21295846]

Frederich RC, Hamann A, Anderson S, Lollmann B, Lowell BB, Flier JS. Leptin levels reflect body lipid content in mice: evidence for diet-induced resistance to leptin action. Nature medicine. 1995; 1:1311–1314.

Friedman JM. Modern science versus the stigma of obesity. Nature medicine. 2004; 10:563–569.

Friedman JM. Leptin at 14 y of age: an ongoing story. The American journal of clinical nutrition. 2009; 89:973S–979S. [PubMed: 19190071]

Halaas JL, Boozer C, Blair-West J, Fidahusein N, Denton DA, Friedman JM. Physiological response to long-term peripheral and central leptin infusion in lean and obese mice. Proceedings of the National Academy of Sciences of the United States of America. 1997; 94:8878–8883. [PubMed: 9238071]

Halaas JL, Gajiwala KS, Maffei M, Cohen SL, Chait BT, Rabinowitz D, Lallone RL, Burley SK, Friedman JM. Weight-reducing effects of the plasma protein encoded by the obese gene. Science. 1995; 269:543–546. [PubMed: 7624777]

Hieronymus H, Lamb J, Ross KN, Peng XP, Clement C, Rodina A, Nieto M, Du J, Stegmaier K, Raj SM, et al. Gene expression signature-based chemical genomic prediction identifies a novel class of HSP90 pathway modulators. Cancer cell. 2006; 10:321–330. [PubMed: 17010675]

Kelly T, Yang W, Chen CS, Reynolds K, He J. Global burden of obesity in 2005 and projections to 2030. International journal of obesity. 2008; 32:1431–1437. [PubMed: 18607383]

Lamb J, Crawford ED, Peck D, Modell JW, Blat IC, Wrobel MJ, Lerner J, Brunet JP, Subramanian A, Ross KN, et al. The Connectivity Map: using gene-expression signatures to connect small molecules, genes, and disease. Science. 2006; 313:1929–1935. [PubMed: 17008526]

Lee J, Ozcan U. Unfolded protein response signaling and metabolic diseases. The Journal of biological chemistry. 2014; 289:1203–1211. [PubMed: 24324257]

Lee JH, Koo TH, Yoon H, Jung HS, Jin HZ, Lee K, Hong YS, Lee JJ. Inhibition of NF-kappa B activation through targeting I kappa B kinase by celastrol, a quinone methide triterpenoid. Biochemical pharmacology. 2006; 72:1311–1321. [PubMed: 16984800]

Liou AP, Paziuk M, Luevano JM Jr, Machineni S, Turnbaugh PJ, Kaplan LM. Conserved shifts in the gut microbiota due to gastric bypass reduce host weight and adiposity. Science translational medicine. 2013; 5:178ra141.

Mokadem M, Zechner JF, Margolskee RF, Drucker DJ, Aguirre V. Effects of Roux-en-Y gastric bypass on energy and glucose homeostasis are preserved in two mouse models of functional glucagon-like peptide-1 deficiency. Molecular metabolism. 2014; 3:191–201. [PubMed: 24634822]

Myers MG Jr, Leibel RL, Seeley RJ, Schwartz MW. Obesity and leptin resistance: distinguishing cause from effect. Trends in endocrinology and metabolism: TEM. 2010; 21:643–651. [PubMed: 20846876]

Neckers L. Heat shock protein 90: the cancer chaperone. Journal of biosciences. 2007; 32:517–530. [PubMed: 17536171]

Olshansky SJ, Passaro DJ, Hershow RC, Layden J, Carnes BA, Brody J, Hayflick L, Butler RN, Allison DB, Ludwig DS. A potential decline in life expectancy in the United States in the 21st century. The New England journal of medicine. 2005; 352:1138–1145. [PubMed: 15784668]

Ozcan L, Ergin AS, Lu A, Chung J, Sarkar S, Nie D, Myers MG Jr, Ozcan U. Endoplasmic reticulum stress plays a central role in development of leptin resistance. Cell metabolism. 2009; 9:35–51. [PubMed: 19117545]

Ozcan U, Cao Q, Yilmaz E, Lee AH, Iwakoshi NN, Ozdelen E, Tuncman G, Gorgun C, Glimcher LH, Hotamisligil GS. Endoplasmic reticulum stress links obesity, insulin action, and type 2 diabetes. Science. 2004; 306:457–461. [PubMed: 15486293]

Ozcan U, Ozcan L, Yilmaz E, Duvel K, Sahin M, Manning BD, Hotamisligil GS. Loss of the tuberous sclerosis complex tumor suppressors triggers the unfolded protein response to regulate insulin signaling and apoptosis. Molecular cell. 2008; 29:541–551. [PubMed: 18342602]

Ozcan U, Yilmaz E, Ozcan L, Furuhashi M, Vaillancourt E, Smith RO, Gorgun CZ, Hotamisligil GS. Chemical chaperones reduce ER stress and restore glucose homeostasis in a mouse model of type 2 diabetes. Science. 2006; 313:1137–1140. [PubMed: 16931765]

Park SW, Ozcan U. Potential for therapeutic manipulation of the UPR in disease. Seminars in immunopathology. 2013; 35:351–373. [PubMed: 23572207]

Park SW, Zhou Y, Lee J, Lee J, Ozcan U. Sarco(endo)plasmic reticulum Ca2+-ATPase 2b is a major regulator of endoplasmic reticulum stress and glucose homeostasis in obesity. Proceedings of the National Academy of Sciences of the United States of America. 2010; 107:19320–19325. [PubMed: 20974941]

Ron D, Walter P. Signal integration in the endoplasmic reticulum unfolded protein response. Nature reviews Molecular cell biology. 2007; 8:519–529. [PubMed: 17565364]

Ryan KK, Tremaroli V, Clemmensen C, Kovatcheva-Datchary P, Myronovych A, Karns R, Wilson-Perez HE, Sandoval DA, Kohli R, Backhed F, et al. FXR is a molecular target for the effects of vertical sleeve gastrectomy. Nature. 2014; 509:183–188. [PubMed: 24670636]

Williams KW, Liu T, Kong X, Fukuda M, Deng Y, Berglund ED, Deng Z, Gao Y, Liu T, Sohn JW, et al. Xbp1s in Pomc Neurons Connects ER Stress with Energy Balance and Glucose Homeostasis. Cell metabolism. 2014

Zhang Y, Proenca R, Maffei M, Barone M, Leopold L, Friedman JM. Positional cloning of the mouse obese gene and its human homologue. Nature. 1994; 372:425–432. [PubMed: 7984236]

HIGHLIGHTS

- Celastrol is a natural compound extracted from Thunder of God Vine.
- Celastrol creates similar expression profile to those of reduced ER stress conditions.
- Celastrol is a powerful leptin sensitizer.
- Celastrol has potential as an anti-obesity therapeutic agent.

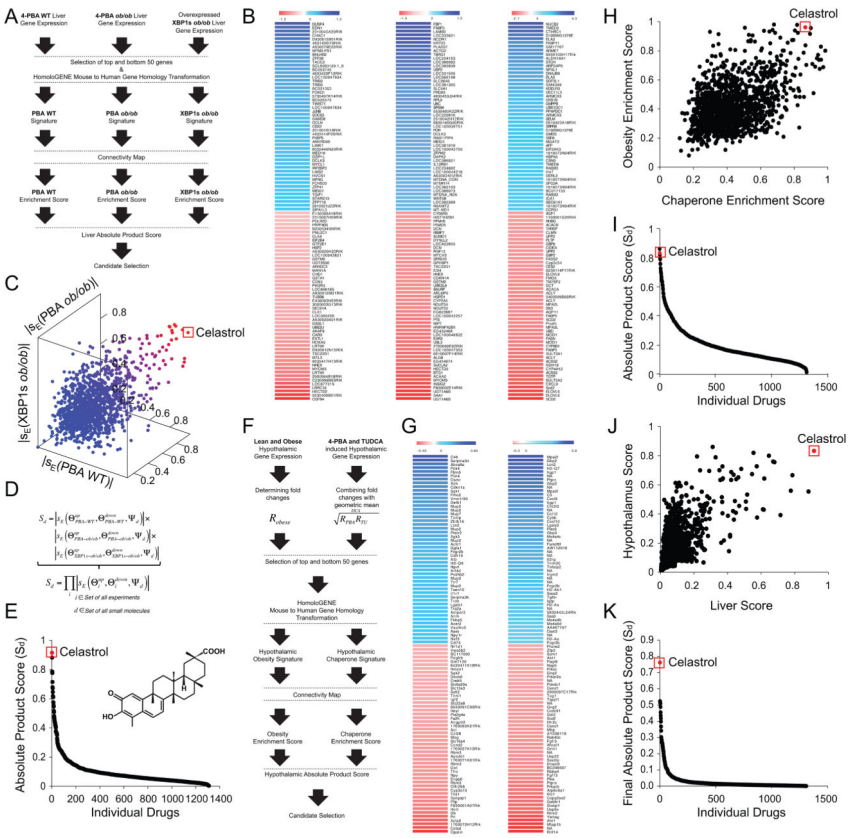

Figure 1. Identification of Celastrol as a Potential Anti-Obesity Molecule

(A) Flow chart depicting the process for obtaining gene expression signatures from the liver to identify potential anti-obesity compounds. C57BL/6J mice (left flow chart) or *ob/ob* mice (middle flow chart) were orally treated with either vehicle or 4-PBA (n=3 for each group) and *ob/ob* mice injected with Ad-XBP1s or Ad-LacZ (n=3 for each group) (right flow chart). **(B)** Heat maps representing the selected 50 upregulated (blue) and 50 downregulated (red) genes – vehicle versus 4-PBA from lean mice (left), vehicle versus 4-PBA from *ob/ob* mice (middle) and Ad-XBP1s versus Ad-LacZ from *ob/ob* mice (right). Microarray chip probe and the corresponding gene identifiers are listed next to the heat maps. **(C)** Three dimensional plot of the absolute enrichment scores obtained from CMAP using three different signatures. Each data point represents a small molecule. Blue to red color-codings represent low to high absolute product score. **(D)** Formula used to calculate absolute enrichment score for individual small molecules in CMAP database. **(E)** Distribution of the calculated absolute enrichment score of individual small molecules. The red dot represents Celastrol and its chemical structure is shown in the graph. **(F)** Flow chart depicting the process used to obtain gene expression signatures in the hypothalamus. C57BL/6J mice were fed on either normal chow diet or high fat diet (n=4 for each group) (left flow chart). DIO mice treated with either vehicle, or 4-PBA or with TUDCA (right flow chart). Geometric means of 4-PBA and TUDCA-induced changes in gene expression (R_{PBA} and R_{TUDCA}) were determined to obtain hypothalamic chaperone signature. **(G)** Heat map representing the selected 50 upregulated and 50 downregulated hypothalamic genes obtained. Left: lean

versus DIO. Right: Vehicle versus (4-PBA and TUDCA). **(H)** Distribution of individual small molecules in CMAP depending on their absolute enrichment scores obtained by analysis of hypothalamic obesity signature (Y-axis: obesity enrichment score) and hypothalamic chaperone signature (X-axis: chaperone enrichment score). **(I)** Distribution of hypothalamic absolute product scores of individual small molecules obtained from CMAP database. **(J)** The dot distribution of absolute product scores of the liver and the hypothalamus. Each data point represents an individual small molecule. **(K)** Distribution of the final scores calculated as a product of liver and hypothalamus absolute product scores. Red dot represents Celastrol (**H–K**). See also Figure S1.

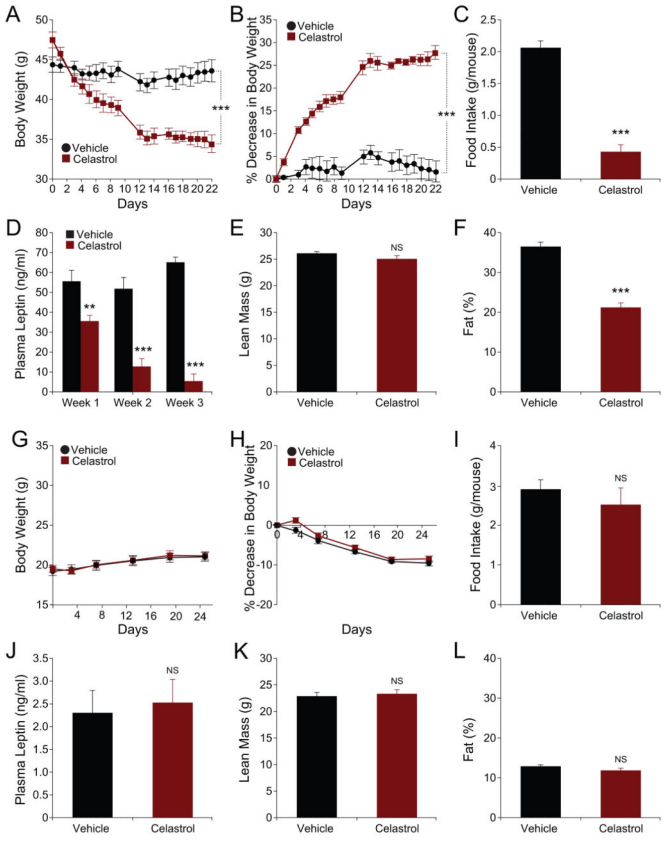

Figure 2. Celastrol Acts as an Anti-Obesity Agent on High Fat Diet-Induced Obese Mice

High fat-fed obese (DIO) mice **(A–F)** or 10-week-old C57BL/6J lean mice **(G–L)** were daily treated with vehicle or Celastrol (100 μg/kg) intraperitoneally (i.p) for three weeks. **(A)** Body weight (g) (n=5 for each group) and **(B)** Percent decrease (%) in body weight in DIO mice during the treatment. **(C)** Three-day average of food intakes (g) of DIO mice during the first week of treatment. Experiments were repeated in more than three independent cohorts. **(D)** Plasma leptin levels of vehicle (n=8) or Celastrol (n=8; 100 μg/kg)-treated DIO mice during three weeks of treatment. **(E–F)** Dual energy X-ray absorptiometry (DEXA) scans showing **(E)** lean mass (g) and **(F)** fat mass (%) of DIO mice after three weeks of treatment (n=6 per each group). DEXA scans were repeated in more than three independent cohorts. **(G)** Body weight (g) (n=5 for each group), and **(H)** percent decrease (%) in body weight of lean mice during the treatment. **(I)** Three-day average food intakes of the lean mice during the first week of treatment. Experiments in **(G–I)** were repeated three times. **(J)** Plasma leptin levels of lean mice after three week of treatment (n=11 for each group). **(K)** Lean mass (g) and **(L)** fat mass percent (%) of lean mice after three weeks treatment (n=6 per each group). Error bars are represented as mean ± SEM. p values were determined by two-way ANOVA (**A and B**) or Student's t test (*p < 0.05, **p < 0.01, ***p <0.001). See also Figure S2 and S7.

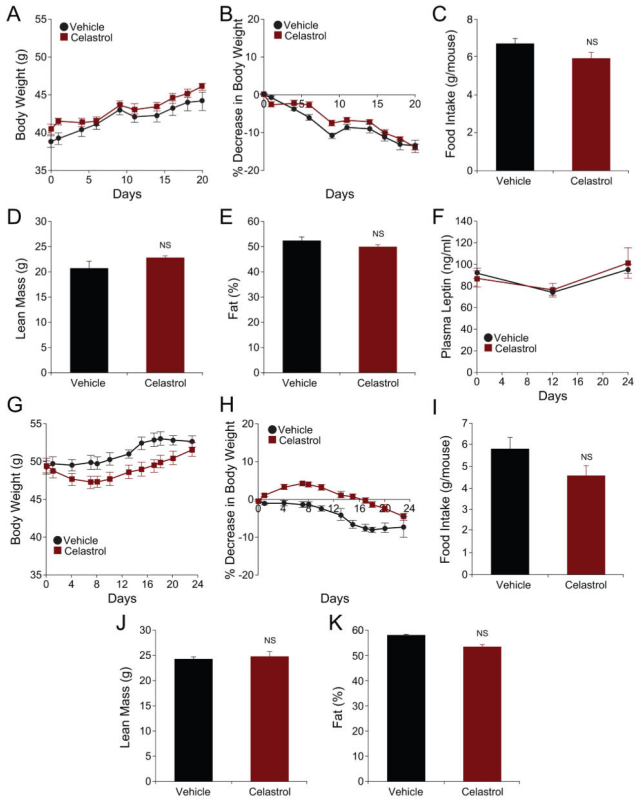

Figure 3. Celastrol Is Minimally Effective in *db/db* or *ob/ob* Mice

Eight-week-old male *db/db* **(A–F)** or *ob/ob* mice **(G–K)** were subjected to a three-week treatment of vehicle or Celastrol (100 μg/kg) (daily, i.p.). **(A)** Body weight (g) and **(B)** percent decrease in bodyweight of *db/db* mice during the treatment (n=5 for each group). **(C)** three-day average of food intakes of *db/db* mice during the first week of treatment. Experiments were repeated in three independent cohorts. **(D)** Lean mass (g) and **(E)** fat percentage (%) of *db/db* mice determined by DEXA scans after three weeks treatment (n=5 for each group). DEXA scans were done on two different cohorts. **(F)** Plasma leptin levels before, 12 and 24 days after Celastrol treatment (n=5 for each group). **(G)** Body weight (g) and **(H)** percent decrease in bodyweight of *ob/ob* mice during the treatment (n=8 for vehicle and n=10 for Celastrol group). **(I)** Three-day average of food intakes of *ob/ob* mice during the second week of the treatment. **(J)** Lean mass (g) and **(K)** fat percentage (%) on three weeks of treatment (n=6 for vehicle and n=5 for Celastrol group) measured by DEXA scan. DEXA scans were performed in two different cohorts. Error bars are represented as mean ± SEM. p values were determined by Student's t test. See also Figure S2 and S7.

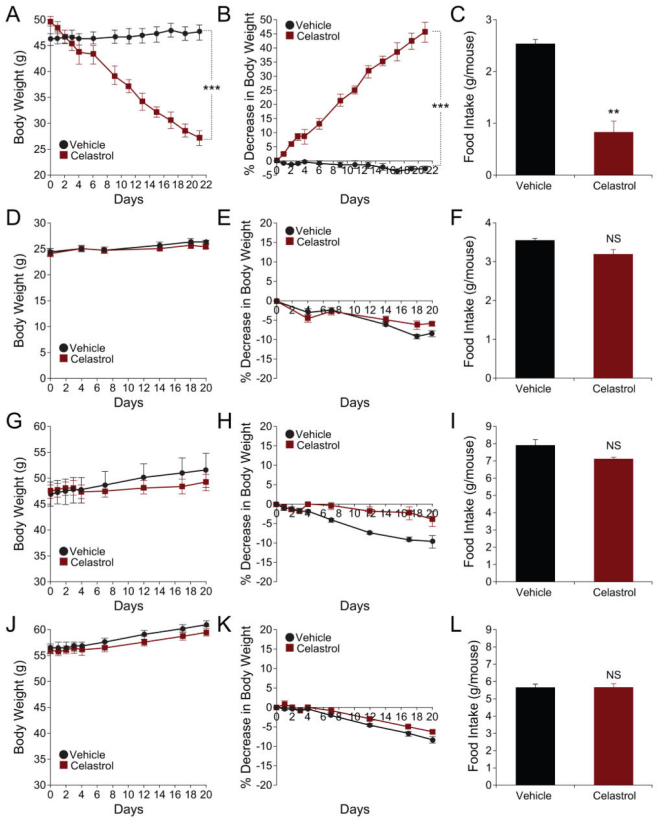

Figure 4. Oral Administration of Celastrol Reduces Body Weight and Food Intake of DIO Mice

(A–C) DIO mice, **(D–F)** lean mice, **(G–I)** *db/db* or **(J–L)** *ob/ob* mice were subjected to oral administration of vehicle (captisol) or Celastrol (10 mg/kg) for three weeks. **(A)** Body weight (g) and **(B)** percent decrease (%) in body weight of DIO mice during the treatment. **(C)** The average of three-day food intakes of DIO mice during the first week of treatment. (n=5 for vehicle group and n=4 for Celastrol group in **(A–C)**). Experiments on DIO mice were independently repeated twice. **(D)** Body weight (g) and **(E)** percent decrease in body weight of lean mice during Celastrol treatment. **(F)** The averages of three-day food intakes (g) of the lean mice during the first week of treatment. N=5 for each group in **(D–F). (G)** Body weight (g) and **(H)** percent decrease in body weight of *db/db* mice during the treatment. **(I)** The average of three-day food intake of *db/db* mice during the first week of treatment. (n=4 for vehicle and n=5 for Celastrol treatment in **(G–I). (J)** Body weight (g) and **(K)** percent decrease in body weight of *ob/ob* mice during Celastrol treatment. **(L)** The average of three-day food intake (g) of *ob/ob* mice during the first week of treatment (N=5 for each group in **(J–L)**). Error bars are represented as mean ± SEM. p values were determined by two-way ANOVA (**A and B**) or Student's t test (*p < 0.05, **p < 0.01, ***p < 0.001).

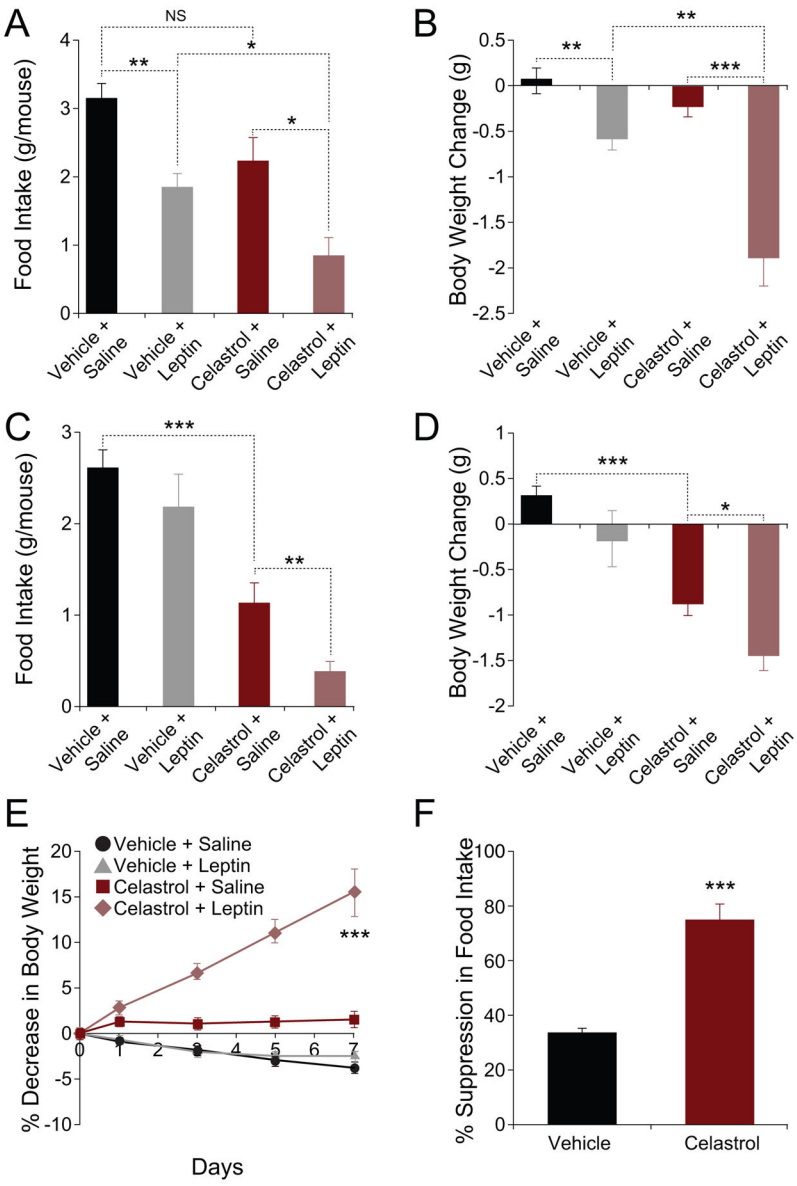

Figure 5. Celastrol Acts as a Leptin Sensitizer

(A and B) Vehicle or Celastrol (150 μg/kg) were administered to lean mice for two days and each group was subsequently received either saline (n=9 for vehicle and n=11 for Celastrol subgroup) or leptin (n=12 for each subgroup) (5 mg/kg). **(A)** Food intake and **(B)** body weight change during 24-hour period following saline/leptin injections. Experiments were repeated in two independent cohorts**. (C and D)** Vehicle (n=12) or Celastrol (n=10; 150 μg/kg) were administered to DIO mice for two days and each group of mice was received either saline (n=6 vehicle; n=5 Celastrol) or leptin (n=6 vehicle; n=5 Celastrol) (1 mg/kg). **(C)** Food intake (g) and **(D)** body weight change (g) during 16-hour period following saline/leptin injections. These experiments were independently repeated two times. **(E and F)** *ob/ob* mice were treated with either vehicle (n=9) or Celastrol (100 μg/kg, n=9) for the next five days. For the next one week, each group of mice was also treated with either saline or

leptin (0.1 mg/kg) (n=5 saline and n=4 leptin). **(E)** Percent decrease in body weight. **(F)** Percent suppression of food intake during leptin treatment. Experiments were repeated in two independent cohorts. Error bars are represented as mean ± SEM. p values were determined by Student's t test (*p < 0.05, **p < 0.01, ***p < 0.001).

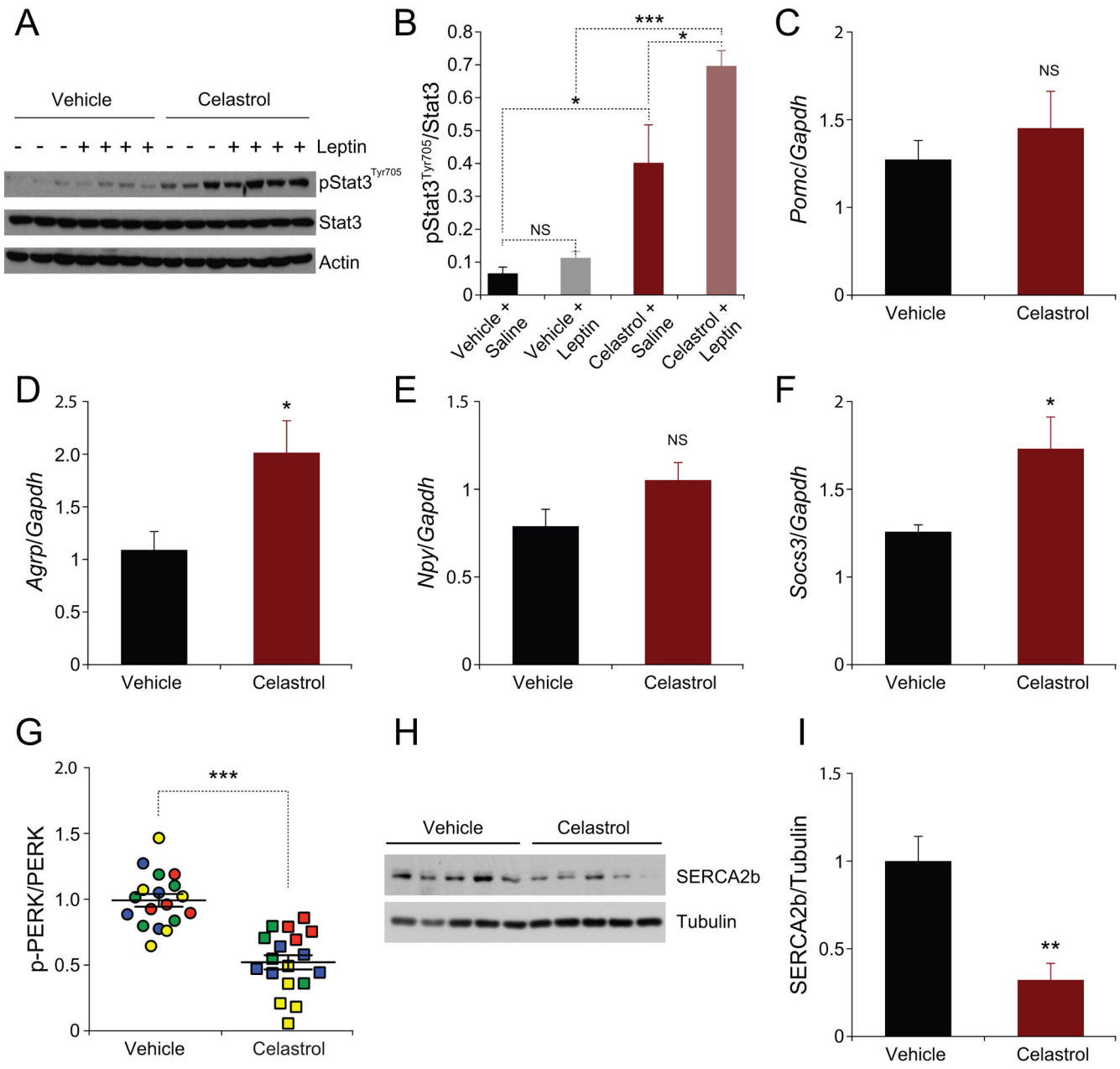

Figure 6. Celastrol Potentiates Leptin Signaling and Reduces ER Stress

(A and B) Vehicle or Celastrol (500 μg/kg) were administered to DIO. 15 hours later, each group of mice was treated with either saline or leptin (1 mg/kg) for 40 minutes. **(A)** Immunoblot analysis of Stat3^{Tyr705} phosphorylation, total Stat3, and actin protein levels from the hypothalamus **(B)** Ratio of signal intensities of pStat^{Tyr705} to total Stat3. **(C–F)** DIO mice were treated with Celastrol (100 μg/kg) or vehicle by i.p. injection daily for four days. **(C)** *Pomc*, **(D)** *Agrp*, **(E)** *Npy* and **(F)** *Socs3* mRNA expression in the hypothalamus. **(G–I)** DIO mice were administered with Celastrol (100 μg/kg) or vehicle (i.p., daily) for three days. On the fourth day, 100 or 250 μg/kg of Celastrol or vehicle was administered six hours before the hypothalamus was collected. **(G)** The quantified ratio of the signals of

phosphorylated PERK (Thr980) to total PERK of the hypothalamus samples from four independent experiments in Figure S3A–H. **(H)** SERCA2b and tubulin protein levels and **(I)** quantified signal intensity of SERCA2b to tubulin. Results in **(G–I)** were independently reproduced in four different cohorts. Error bars are represented as mean ± SEM. p values were determined by Student's t test (*$p < 0.05$, **$p < 0.01$, ***$p < 0.001$). See also Figure S3 and S4.

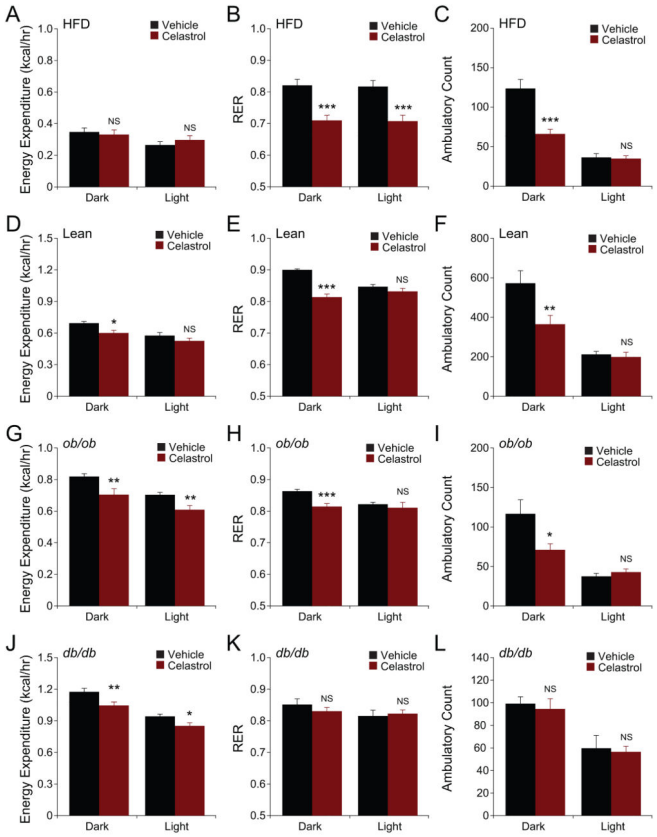

Figure 7. Effect of Celastrol on Metabolic Measures

(A–C) DIO mice, **(D–E)** lean, **(G–I)** *ob/ob* or **(J–L)** *db/db* mice were placed into metabolic cages and received Celastrol (100 μg/kg) or vehicle once a day for three days. **(A, D, G, J)** Energy expenditure, **(B, E, H, K)** respiratory exchange ratios (RER; VCO_2/VO_2), and **(C, F, I, L)** ambulatory count (physical activity) from each group of mice are shown. Bar graphs represent average of two dark (24–36h and 48–60h) and two light cycles (12–24h and 36–48h). Data represented in Figure 7A–C are average of three independent cohorts. (For DIO mice, n=16 for vehicle and n=13 for Celastrol). For data and analysis for Figure 7A–C, see Supplemental Data S1. Data represented in Figure 7D–F are average of two independent cohorts (n=8 for vehicle and Celastrol). For *ob/ob* mice, n=4 for vehicle and Celastrol; for *db/db* mice, n=4 for vehicle and Celastrol). Error bars are represented as mean ± SEM. p values were determined by Student's t test (*$p < 0.05$, **$p < 0.01$, ***$p < 0.001$). See also Figure S5 and S6.